NASA TECHNICAL TRANSLATION

NASA TT, F-14,295

EXPERIMENT ON EXHAUST MUFFLER BY PULSATING AIR FLOW

S. Fujimoto

(NASA-TT-F-14295) EXPERIMENT ON EXHAUST MUFFLER BY PULSATING AIR FLOW S. Fujimoto (Scientific Translation Service) 27 p Jun. 1972
CSCL 20D

N72-26234

G3/12 Unclas 31682

Translation of "Haiki shoonki no kanketsu kiryu jikken," The Journal of the Acoustical Society of Japan (Nihon onkyo gakkai shi), Vol. 27, No. 11, 1971, pp 568-578

NATIONAL AERONAUTICS AND SPACE ADMINISTRATION
WASHINGTON, D.C. 20546 JUNE 1972

EXPERIMENT ON EXHAUST MUFFLER BY PULSATING AIR FLOW*

Shigeo Fujimoto**

ABSTRACT. This paper deals with the silencing effect of exhaust mufflers of automobiles. The purpose of this experiment is especially to investigate the effect of the flow rate of exhaust gas on the changes in noise attenuation in mufflers from the practical point of view. Ten fundamental types of reactive mufflers are tested by an engine, which has a cylinder volume of about 900 cc. The results are compared with those of a test by pulsating air flow at various flow rates.

The spectrum of noises in the pulsating flow test is similar to that of exhaust noises by the engine test as shown in Figure 1. But in general, the sound level in the pulsating flow test is lower in the low frequency range, but higher in the high frequency range than the level in the engine test (Figure 2). The noise attenuation L_e (Equation 1) in the engine test varies with engine load, and is generally in value under the full load than in no load condition, especially in the high frequency range above about 300 Hz (Figure 4). These tendencies are observed clearly in the case of the mufflers with the inlet and outlet pipes installed straight through. The noise attenuation L_p in the pulsating flow test also decreases with an increase in flow rate (Figure 4).

/568***

---

*Received May 17, 1971

**Mechanical Engineering Laboratory, Industrial Technology Agency.

***Numbers in the margin indicate pagination in the original foreign text.

With the noise spectrum divided into two frequency ranges, the low and high frequencies bounded by 500 or 1,000 Hz, the acoustic power of the exhaust noise W' is classified in terms of a function of the mean flow rate as shown in Equations 2 - 5. The acoustic powers, W_L and W_H, of exhaust noises from an exhaust pipe without a muffler consist of the components proportional to the 2nd, 4th or 6th power of the mean flow rate as shown in Figure 5. And the acoustic power W_m of noises generated in a muffler can be explained in terms of the component proportional to the 6th power of the flow rate (Figure 6). The noise attenuation in a muffler is expressed as shown in Equation 8. The amount of attenuation L in a muffler is comparable between the engine test and the pulsating flow test under the condition expressed by Equation 10 (Figure 9). In this case the coefficient of correlation between the results of both tests is given as about 0.78 for the whole muffler (Figure 10).

1. Introduction

A great many research studies have been published, and comparative studies have been made concerning acoustical theory, acoustical experiments [1, 2, 3] or engine experiments [4, 5, 6] about exhaust mufflers for internal combustion engines. The biggest difference between engine experiments and acoustical experiments is the presence of high pressure amplitude [7, 8] and high-speed air flow [9]. The purpose of this report was to establish experimentally the influence of air flow on the silencing effect of automobile mufflers. For this purpose, engine experiments were carried out for ten different muffler elements, and the results were compared, especially for the high frequency range, chiefly with the results of experiments using pulsating air flow [10, 11, 12, 13, 14]. Studies were conducted from the practical viewpoint concerning the influence of the air flow on the silencing effect and concerning the mutual connection between both of the experiments [15, 16, 17].

2. Method of Testing the Test Equipment

2.1. Engine Tested. A four-cylinder, four-cycle gasoline engine of the 900 cc class was used as the engine. An exhaust pipe about 3 m long with an inner diameter of 3 cm was connected to this engine, and this was introduced into an anechoic room. The muffler and tail pipe (about 6 cm long) were attached to the end of this, and the exhaust sound was measured.

2.2. Pulsating Air Flow Testing Equipment. A pressure tank (5 kg/cm^2) was used as the pressure source. It was connected by a pipe to the inlet of the siren device, a pulsating air flow was generated, and it was connected from the siren outlet to the exhaust pipe system (also including the exhaust manifold). There are two types of siren devices: the rotary valve type [10, 13] and the rotary disk type [18]; in these experiments, the latter was used. The rotary disk type is one in which eight rectangular slits are provided in the circumference of a rotating disk. It is constructed so that the air flow passes through when the slits overlap with the siren outlet pipe. The ratio of the slit opening period in one slit opening and closing period in this case is 0.44 (see Appendix I).

In pulsating air flow devices, the length of the pipe connecting the pressure source and the siren inlet has an influence on the flow rate characteristics and the exhaust sound spectrum (a sort of pulsating effect [19]). In these experiments this length was made as short as possible (see Appendix III). /570

2.3. Test Method. The engine tests were performed chiefly at a full load of 2,000 rpm and at no load. The pulsating air flow tests were carried out by adjusting the pulse exhaust frequency of the siren to the fundamental frequency (68 Hz) of these exhausts. All of the exhaust pipe system and mufflers used in the testing were the same as those tested in the engine tests (the same applies also to acoustical tests).

The exhaust sound was measured by putting a condenser microphone obliquely at 50 cm from the exhaust outlet. The exhaust gas temperature in the engine tests was measured by a thermocouple thermometer at the exhaust pipe inlet and in the pipe near the exhaust outlet; the mean value of both of these was taken as the representative value of the exhaust gas temperature. Next, in measuring the flow rate, both a hot wire anemometer and a laminar flow type flow meter were used together. In the pulsating air flow tests, the measuring positions were the exhaust pipe outlet and inlet. In the engine tests, measurements were taken at the inlet part of the air inlet pipe. The mean hourly flow velocity at these positions was measured. (In addition, a hollow container of about 140 liters was connected to the exhaust outlet during measurements only; a Pitot tube was inserted inside the outlet tube of this container, and measurements were attempted of the mean flow velocity.) The measured values of the mean flow velocity were converted into the flow velocity inside the exhaust pipe by using the ratio between the temperature at that position and the above-mentioned representative value of the mean temperature. These flow velocities and temperatures vary depending on the time and place, but it was decided to indicate the state of the exhaust gas by practical representative values and to organize the experimental values (that is, the mean flow velocity, the mean temperature, and the mean density).

In addition to this, the back pressure when each of the mufflers was installed was measured by means of a water column manometer at the exhaust pipe inlet in accordance with the JIS prescriptions.

3. Exhaust Sound Spectrum

Examples of the results of exhaust pipe measurements in engine tests and pulsating air flow tests are shown in Figure 1. These results are those obtained with the exhaust manifold and the exhaust pipe only, with no mufflers; below, this is called the "direct pipe." It is clear from the figure that the exhaust sound spectrum can be divided up into two noise groups.

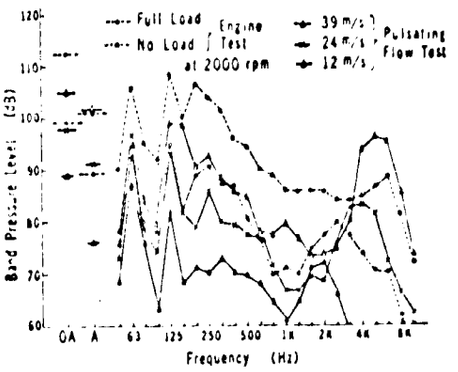

Figure 1. Spectrums of the exhaust noise measured at a distance of 50 cm from the exhaust outlets (without muffler).

The first group has its chief components in the low frequency range, with the exhaust peaks at 68, 130, and 200 Hz. The second group has its chief components in the high frequency range of about 2 kHz or more. Since the peaks in this high frequency range have increases of their frequencies and levels together with increases in the mean flow velocity of the pulsating air flow, it is assumed that the air flow noise is related to the flow velocity in the pipe system. However, it is clear that the level increase in the low frequency range and the high frequency range is different in the engine tests and in the pulsating air flow tests.

This exhaust sound spectrum was divided into a low frequency range and a high frequency range, adopting 500 -1,000 Hz as the boundary, and the full acoustic power in each range was sought. The results are shown in Figure 2 in relation to the mean flow velocity. It is clear from the figure that in the low frequency range there is a higher level in the engine tests, while in the high frequency range there is a greater proportion of level increase in the pulsating air flow tests. Consequently, it may be quite difficult to make the absolute values for the spectra in both tests coincide throughout all the ranges.

4. Attenuation of Mufflers

The muffler elements tested are shown in Figure 3. The A group in the figure are hollow type mufflers. In each of the four, the only differences are the mounting positions of the inlet and outlet pipes (B is a variant of

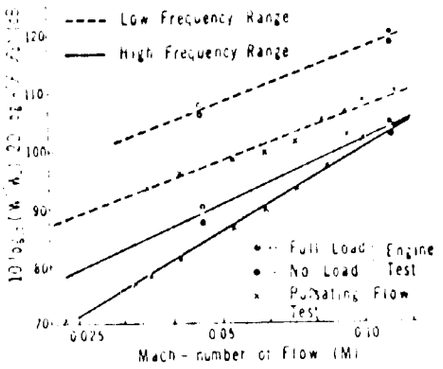

Figure 2. Increase of the exhaust noise (without muffler) as a function of the mean flow rate M in the engine test and the pulsating flow test.

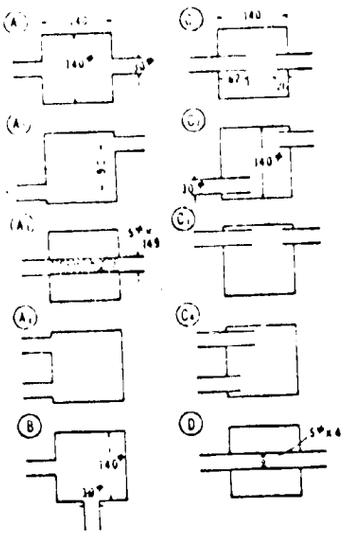

Figure 3. Test mufflers

/571

this). The C group is of the inserted pipe type, using pipes with one-half or one-fourth length. Four different types, with different positions of the inlet and outlet pipes, were prepared. D is the resonator type (the resonance frequency is about 125 Hz).

Table 1 shows the level differences (attenuation) of the noise levels of the mufflers in the engine tests from those of the "direct pipe" results. Generally speaking, the attenuation is lower at full load than at no load. One can assume, in particular, that the A characteristics have a smaller value and that the attenuation in the high frequency range has decreased.

TABLE 1. NOISE LEVEL REDUCTION L_e OF MUFFLERS AT 2,000 rpm OF ENGINE.

condition	dB	A_1	A_2	A_3	A_4	B	C_1	C_2	C_3	C_4	D
full load (400°C, 38 m/s)	C	0	2	1	3	0	1	4	1	0	1
	A	3	6	2	8	6	2	6	3	6	3
no load (200°C, 16 m/s)	C	0	0	0	1	0	0	0	0	2	1
	A	6	4	7	5	5	10	7	9	7	4

In order to clarify this phenomenon, we show in Figure 4 the attenuation caused by 1/3 octave band noise. The attenuation here is defined by the following equation:

$$L = 20\log_{10}(P'/P_0) - 20\log_{10}(P/P_0), \\ = 10\log_{10}(W'/W_0) - 10\log_{10}(W/W_0), \text{(dB)} \qquad (1)$$

L : attenuation (dB)

P': direct pipe sound pressure

P_0: standard sound pressure, 0.0002 μBr

P : sound pressure with muffler attached

W': direct pipe acoustic power

W_0: standard acoustic power, 10^{-12} watt

W: acoustic power with muffler attached

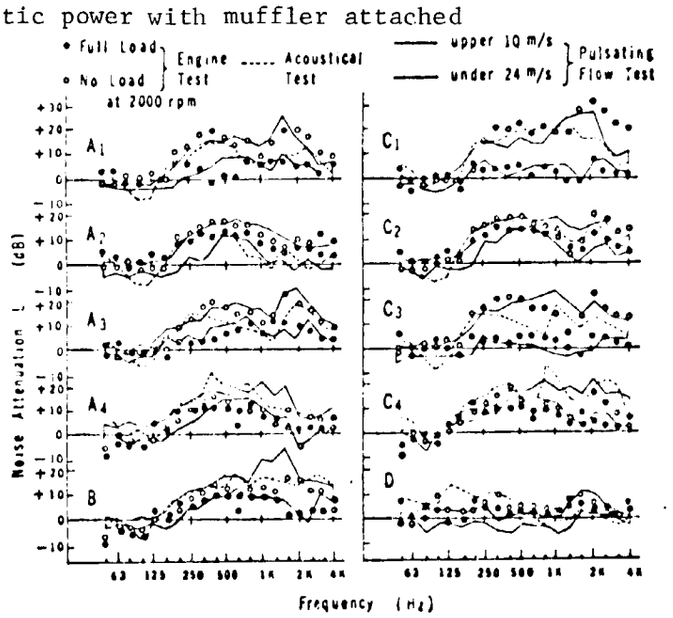

Figure 4. Comparison of the noise attenuation of mufflers in the engine test, the acoustical test and the pulsating flow test.

According to the figure, in engine tests the attenuation is smaller at full load than at no load, especially in the frequencies of about 250 Hz or more. This tendency is pronounced in cases when the positions of the inlet and outlet pipes are opposite each other, such as A_1, C_1 and C_3. In

the engine tests, the attenuation appears to be concentrated around the frequencies at room temperature with respect to the increment in the sound speed caused by the temperature inside the pipe. Next, the attenuation during the pulsating air flow tests is indicated by the width when the mean flow velocity is 10 m/s or 24 m/s. In this case also, the attenuation tends to become smaller when there is a greater flow velocity. The acoustic test /572
values in the figure are those using 1/3 octave band noise (see Appendix I). It is clear that the values for no load in the engine tests and the 10 m/s values for the pulsating air flow tests more or less agree. (In cases when the load and the flow velocity are great, attenuation decreases are observed particularly in the medium or higher frequencies in cases when the representative component frequency of the air flow noise, f, is $f = S \times \bar{v}/d$). S represents the Strouhal number, $\bar{v}$ — the mean flow velocity, and d — the representative dimensions. Thus, if the pipe diameter d is small, f will be greater. Consequently, if the exhaust pipe dimensions are great, f will have an influence on even lower areas.

5. Power of Exhaust Sound and Flow Velocity

As for aerodynamic noise, the noise characteristics are classified and organized according to the nature of the sound source [21, 22, 23]. Let us now apply this concept to exhaust sounds. In general, the amount of noise generated (see Appendix IV) can be indicated in the following terms:

$$W_n = K_n \rho^2 v^{2n} A / \rho_0 C_0^{2n-3} = K_n \rho^2 C_0^3 M^{2n} A / \rho_0 \quad \text{(watt)} \tag{2}$$

W_n: acoustic power

ρ : sound source air density

ρ_0: atmospheric density

$\bar{v}$: mean flow velocity

C_0: sound velocity in the atmosphere

A : area of exhaust outlet

M : $\bar{v}/C_0$: Mach number for sound velocity in the atmosphere

K_n: non-dimensional coefficient,

n : index, 1 - 4

In this case, n = 1 in cases when there is an extremely low velocity $\bar{v}$. This corresponds to linear acoustical theory (constant velocity sound source) [24]. When external forces operate with a boiling point type sound source, n = 2, and when they operate with a pressure noise source, n = 3. n = 4 applies to turbulence noise, which is known as jet noise [21, 22]. In exhaust noise, when the mean flow velocity is low, n = 1. Normally this is assumed to be a pulsating boiling point sound source. Air flow noise caused by pipe walls or protrusions in the exhaust pipe or muffler corresponds to n = 3.

Transforming Equation (2), we obtain:

$$\begin{aligned} PWL_n &= 10 \log_{10}(W_n/W_0) \\ &= 10 \log_{10} k_n + 10 \log_{10}(A/A_0) \\ &\quad + 20 \log_{10}(\rho/\rho_0) + 20 \log_{10} M^n, \text{ (dB)} \end{aligned} \tag{3}$$

Here, PWL_n: power level (dB)

A_0 : standard area, 1 m^2

k_n : $K_n \rho C_0^3 A_0/W_0$: acoustic power coefficient (non-dimensional)

Let us now organize the values from pulsating air flow tests, given in Figure 2, into the low frequency range and the high frequency range, on the basis of the above-mentioned concept. The results are as shown in Figure 5. It is clear that the low frequency range consists of components of n = 1 and n = 2, while the exhaust sound in the high frequency range consists of components of n = 2 and n = 3 (when the flow velocity doubles, the level increment is 6 dB when n = 1, 12 dB when n = 2, and 18 dB when n = 3). That is, the low frequency range power W_L and the high frequency range power W_H will be:

$$\left.\begin{aligned} 10 \log_{10}(W_L/W_0) &= 10 \log(W_1 + W_2)/W_0, \text{ (dB)} \\ 10 \log_{10}(W_H/W_0) &= 10 \log_{10}(W_2 + W_3)/W_0, \text{ (dB)} \end{aligned}\right\} \tag{4}$$

Here,

$$\left.\begin{aligned} W_L/W_0 &= (\rho/\rho_0)^2(A/A_0)(k_1M^2 + k_2M^4) \\ &\doteqdot (\rho/\rho_0)^2(A/A_0)(k_LM^{2n}) \qquad 1 \leqq n < 2 \\ W_H/W_0 &= (\rho/\rho_0)^2(A/A_0)(k_2M^4 + k_3M^6) \\ &\doteqdot (\rho/\rho_0)^2(A/A_0)(k_HM^{2n}) \qquad 2 \leqq n \leqq 3 \end{aligned}\right\} \tag{5}$$

Table 2 gives the k_n values of the exhaust sound in the "direct pipe" state for pulsating air flow tests and engine tests. In the low frequency range, the engine tests give higher values, but in the high frequency range, the pulsating air flow tests have higher values.

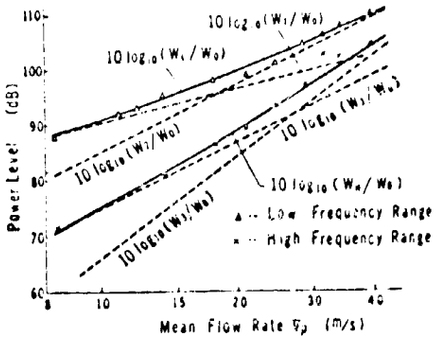

Figure 5. Increase of the exhaust noise W' as a function of the flow rate $\bar{v}_p$ in the pulsating flow test (without muffler).

TABLE 2. ACOUSTIC POWER COEFFICIENT k_n ON EXHAUST NOISE WITHOUT MUFFLER.

range		engine test	pulsating flow test
low freq. (k_L)	$10\log_{10} k_1$	141 dB	132 dB
	$10\log_{10} k_2$	171 dB	158 dB
high freq. (k_H)	$10\log_{10} k_2$	155 dB	148 dB
	$10\log_{10} k_3$	162 dB	169 dB

6. Attenuation and Acoustic Power

As was mentioned above, the attenuation of the muffler is subject to the influence of the flow velocity, especially in the high frequency range. Equation (1) for this attenuation L can be revised as follows to indicate the acoustic power of the preceding section:

$$L = 10\log_{10}(W_H/W_0) - 10\log_{10}(W/W_0) \tag{6}$$

The power of the exhaust sound when the muffler is attached, W, can be expressed as follows:

$$\left.\begin{aligned} W &= (W_H/|D|^2) + W_m \\ W_m/W_0 &= k_m(\rho/\rho_0)^2(A/A_0)M^m \end{aligned}\right\} \quad (7)$$

W_m: acoustic power of the noise produced by the installation of various mufflers (high frequency range)

$20 \log_{10} D = L_a$: pure acoustic attenuation (see Appendix 1) /573

L_a can also be sought by acoustic tests, but here the value sought from pulsating air flow tests at an extremely low velocity is more appropriate. Let us here calculate $10 \log_{10}(W_m/W_0)$ by means of Equations (6) and (7) from the level (high frequency range) in the "direct pipe" state and with various mufflers attached in pulsating air flow tests with the identical mean flow velocity. The results of these calculations are shown in Figure 6. The figure shows that, when the mean flow velocity doubles, the level increases by 18 dB. Assuming that the power m of W_m in Equation (7) is m = 3, it is possible to organize the data in the following manner:

$$W_m/W_0 = (\rho/\rho_0)^2(A/A_0)(k_m M^6) \quad (8)$$

In view of the nature of the air flow noise mentioned above, m = 3 is considered to be a suitable value. Table 3 shows the calculated values of k_m for various mufflers. Generally speaking, the values in the engine tests are on the same level as, or higher than, those in the pulsating air flow tests.

Figure 7 shows examples of two or three mufflers in pulsating air flow tests. It is clear that the rate of increase of the power W of the exhaust sound when mufflers are attached with respect to the flow velocity differs, depending upon the relative magnitude of $W_H/|D|^2$ and W_m in Equation (7). Consequently, there is a larger W_m in mufflers A_1 and C_1, in which there is a great decline of the attenuation due to the increase in the flow velocity. In A_2, in which there is not much of a decline, the explanation is that W_m is smaller than $W_H/|D|^2$.

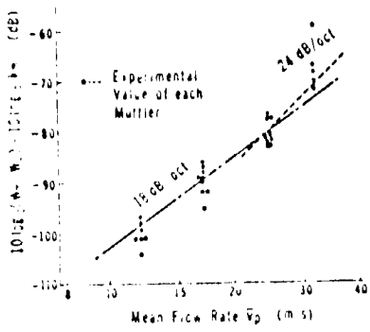

Figure 6. Increase of the noise power W_m generated in the muffler as a function of the flow $\bar{v}_p$ in the pulsating flow test (high frequency range).

TABLE 3. ACOUSTIC POWER COEFFICIENT k_m ON NOISE GENERATED IN MUFFLER (HIGH FREQUENCY).

muffler	$20\log_{10}D$ (dB) acoustical attenuation	$10\log_{10}k_m$ (dB) engine test	pulsating flow test
A_1	10	168	164
A_2	7	165	161
A_3	10	167	162
A_4	12	168	169
B	16	169	162
C_1	18	170	166
C_2	13	168	168
C_3	17	170	167
C_4	13	171	165
D	3	162	155

7. Engine Tests and Pulsating Air Flow Tests

/574

According to the studies up to the preceding section, the attenuation of the muffler (in the high frequency range) will be:

$$\begin{aligned} L &= 10\log_{10}(W_H/W_0) - 10\log_{10}(W/W_0), \\ &\doteqdot 20\log_{10}|D| \\ &\quad - 10\log_{10}(1+(|D|^2 k_m M^{2(m-n)})/(kn)), \\ &\doteqdot L_a - \Delta L \qquad \text{(dB)} \end{aligned} \tag{8}$$

That is, the attenuation L will decrease by an amount proportional to ΔL, the amount of change from the pure acoustic attenuation L_a (unrelated to the flow velocity) caused by the flow velocity. The greater is $|D|^2 k_m/k_H$, the greater will be the magnitude of ΔL. The greater the value of $2(m - n)$, the more sensitive will it be to changes in the flow velocity.

The results in these experiments were:

In engine tests, (a) $m \doteqdot 3$, $n \doteqdot 2.0$,

In air flow tests, (b) $m \doteqdot 3$, $n \doteqdot 2.3$,

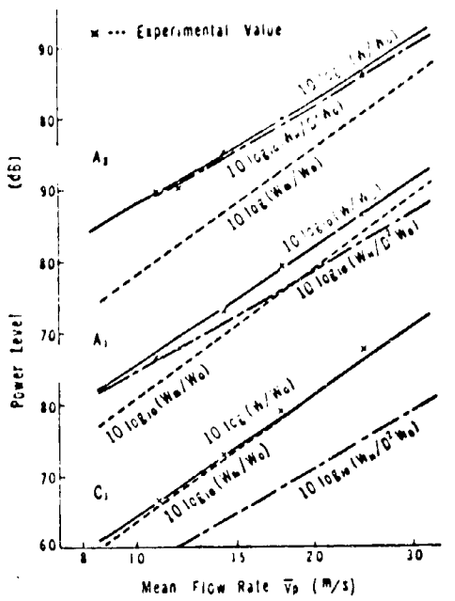

Figure 7. Increase of the exhaust noise power W as a function of the flow rate $\bar{v}_p$ in the pulsating flow test (high frequency range; with muffler A_1, A_2 and C_1).

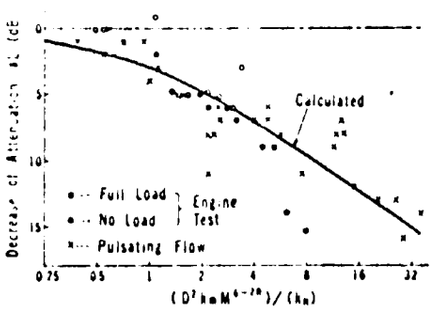

Figure 8. Decreased amounts of the noise attenuation of mufflers (high frequency range).

Figure 8 shows the experimental values sought with respect to $|D|^2 k_m/k_H$ in the engine tests and pulsating air flow tests for the various mufflers. The values for all the different mufflers can more or less be organized by means of Equation (8).

Next, the difference S between the attenuation in the engine tests L_e and the attenuation in the pulsating air flow tests L_p will be as follows (the suffix e indicates engine tests, and the suffix p indicates pulsating air flow tests):

$$L_e - L_p = S = 10\log_{10}\{(1+(|D|^2 k_{mp} M_p^{2(n-a)})/k_{Hp})/(1+(|D|^2 k_{me} M_e^{2(n-a)})/k_{He})\} \quad (9)$$

Consequently, the following will be the conditions for agreement of the attenuation values for both experiments, when the mean flow velocity is $\bar{v}_e$ and $\bar{v}_p$

$$k_{mp} M_p^{1.4}/k_{Hp} = k_{me} M_e^{2.0}/k_{He} \quad (10)$$

In Figure 9 the experimental values of L_e at full load and at no load, from which the values of L_p (air flow tests) at various flow velocities have been subtracted, are shown with respect to the calculated values of S. Although there is considerable

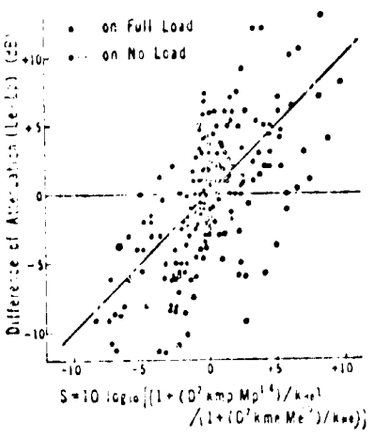

Figure 9. Changes of the values $(L_e - L_p)$ of mufflers as a function of the ratio S.

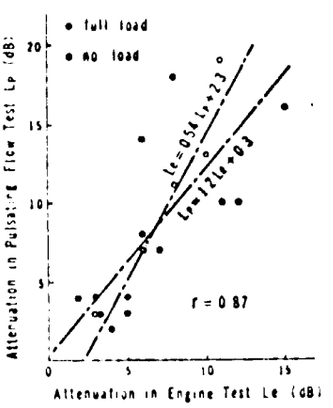

Figure 10. Relation of the noise attenuation L_e in the engine test and L_p in the pulsating flow test under the suitable condition of S = 0.

dispersion, the values more or less are located on the 45° line. As for the mean flow velocity of the air flow tests, $\bar{v}_p$, satisfying Equation (10), there is considerable dispersion depending upon the type of muffler. On an average, at the value of $\bar{v}_e/\bar{v}_p$ the results are about 1.5 at full load, and about 1.9 at no load. That is, in the air flow tests, it is indicated that the experimental values tally at flow velocities lower than those in the engine tests. [The value of $\bar{v}_e/\bar{v}_p$ which satisfies the conditions that the $\rho\bar{v}^2$ values for the exhaust flow should be equal in the engine tests and the air flow tests is 1.5 at full load and 1.3 at no load; these values are close to the values calculated from Equation (10)]. Figure 10 gives the agreement between L_p, the attenuation at flow velocity $\bar{v}_p$ in the pulsating air flow tests satisfying these conditions, and L_e, the attenuation in the engine tests. The correlation coefficient between both was 0.78. It also shows that the regression line is given by

/575

$$L_e = 0.54\ L_n + 2.3\ (dB)$$

$$L_p = 1.2\ L_e + 0.3\ (dB)$$

8. Acoustical Power Coefficient k_n

In the studies up to the preceding section, the exhaust sound and the attenuation were classified and organized in terms of k_n. In Table 4, the values of this k_n are organized for steady flow tests, pulsating flow tests, and engine tests. The pressure coefficient used here is the value of $(\Delta p/\rho v^{-2})$ when Δp is the back pressure, and ρv^{-2} is the dynamic pressure of the exhaust flow. The magnitude of this pressure coefficient indicates the magnitude of the flow resistance for different exhaust pipe systems. Furthermore, it also corresponds to the flow fluctuation intensity in the same exhaust system. Consequently, it has the smallest value during steady flow tests. In steady flow tests, naturally, there is no k_n for the "direct pipe" state in the low frequency range. According to the table, there are larger values of k_n in tests with larger pressure coefficients, but in the k_m related to the noise inside the muffler there is not as great a difference as in the value of k_n related to the exhaust sound itself in the "direct pipe" state. This may be attributed to the following. Whereas the exhaust sound ("direct pipe") varies chiefly on account of the type of sound source (engine, siren), the noise inside the muffler tends to be governed more extensively by the structure of the muffler itself. Consequently, the k_n of the exhaust sound ("direct pipe") differs considerably depending upon the engine. An example of this is shown in Table 5. It is clear that there is a fairly large value with a single cylinder engine. Therefore, it is naturally conceivable that, even with the same muffler, the value of the attenuation L will vary if the engine is different.

9. Conclusion

The studies described above were performed concerning exhaust mufflers, dividing up the acoustic spectrum into a low frequency range and a high frequency range, with 500 - 1,000 Hz as the boundary. The results of the engine tests were compared with the results of pulsating air flow tests. The results of these studies may be summarized as follows.

TABLE 4. RELATION BETWEEN ACOUSTIC POWER COEFFICIENT AND BACK PRESSURE COEFFICIENT (AVERAGED VALUE INCLUDING DATA UNDER SOME OTHER TEST CONDITIONS).

		engine test	pulsating flow test	steady flow test
back pressure coefficient	$20\log_{10}(\Delta p/\rho c^2)$ (dB)	~13.1	~9.8	~8.1
low freq. (k_L)	$10\log_{10} k_1$ (dB)	141~150	130~136	
	$10\log_{10} k_2$ (dB)	171~185	153~164	
high freq. (k_H)	$10\log_{10} k_2$ (dB)	155~180	143~149	128
	$10\log_{10} k_3$ (dB)	162~178	167~174	156
noise in muffler	$10\log_{10} k_m$ (dB)	165~175	161~172	154

TABLE 5. ACOUSTIC POWER COEFFICIENT OF OTHER ENGINES.

		engine under test (3,000 rpm)	other 4 cylinders engine (3,000 rpm)	single cylinder engine (4,000 rpm)
low freq. (k_L)	$10\log_{10} k_1$ (dB)	142	151	161
	$10\log_{10} k_2$ (dB)	163	171	196
high freq. (k_H)	$10\log_{10} k_2$ (dB)	157	161	185
	$10\log_{10} k_3$ (dB)	173	169	215

(1) The pattern of the exhaust sound spectrum is similar in both the engine tests and the pulsating flow tests, but the absolute values of the levels do not necessarily coincide. The level for the engine tests tends to be higher in the low frequency range, and the level for the pulsating flow tests tends to be higher in the high frequency range.

(2) The power of the exhaust sound in the low frequency range consists of components proportional to the second to fourth power of the mean flow velocity. In the high frequency range, it can be expressed in terms of components proportional to the fourth to sixth power. However, the proportions occupied by these components differ in the engine tests and the

pulsating flow tests.

(3) The attenuation of the mufflers (chiefly in the high frequency range) declines together with the increase of the load or of the flow velocity in both engine tests and pulsating flow tests. This decrease in the attenuation is particularly great in mufflers in which the inlet and outlet pipes are located opposite each other. /576

(4) This decline phenomenon can be explained in terms of noise inside the muffler generated in direct proportion to the sixth power of the flow velocity.

(5) The experimental conditions for pulsating flow tests corresponding to the engine tests can be found from the ratio of the generation coefficients of these acoustical powers.

A series of experiments was performed concerning the influence of the flow velocity upon the attenuation of the mufflers, and the above conclusions were reached. Problems still remain concerning the exhaust system, but at least the characteristics of the exhaust sound in the high frequency range and the phenomenon of the attenuation decline were classified and organized from a practical standpoint using the mean flow velocity, and success was achieved in comparing the results with the pulsating flow tests and in making clear the limit conditions.

In conclusion, we heartily thank Professor Igarashi Juichi of the Tokyo University Aerospace Flight Institute, who kindly provided his guidance in carrying out these experiments. We also express our gratitude to specialists Kitada Motokazu and Sakurai Hisao of this laboratory, who collaborated in these experiments.

APPENDIX I. ACOUSTIC TESTS

In the acoustic tests, P is used to represent the sound pressure, U to represent the volume velocity, suffix 0 to represent the sound source, and suffix t to represent the exhaust outlet end. In these tests, the following will hold when the mufflers are attached:

$$\begin{bmatrix} P_0 \\ U_0 \end{bmatrix} = \begin{bmatrix} A_m & B_m \\ C_m & D_m \end{bmatrix} \begin{bmatrix} P_t \\ U_t \end{bmatrix}$$

However, in the "direct pipe" state:

$$\begin{bmatrix} P_0' \\ U_0 \end{bmatrix} = \begin{bmatrix} A' & B' \\ C' & D' \end{bmatrix} \begin{bmatrix} P_t' \\ U_t' \end{bmatrix} \quad \begin{matrix} P_t/U_t \fallingdotseq 0 \\ U_0 \equiv \text{const.} \end{matrix}$$

Consequently, IL, the insertion loss in the exhaust pipe system, will be:

$$IL_m = 20 \log_{10} |U_0/U_t| \fallingdotseq 20 \log_{10} |D_m|$$
$$IL = 20 \log_{10} |U_0/U_t'| \fallingdotseq 20 \log_{10} |D'|$$

The standard muffler attenuation in the "direct pipe" state will be:

$$L_m = 20 \log_{10} |U_t'/U_t|$$
$$= 20 \log_{10} |D'| - 20 \log_{10} |D_m| = 20 \log_{10} |D|$$

In measuring IL, the speaker is put in front of the tail pipe end, the sound source end side is closed. The sound pressure at the tail pipe end P_t and the sound pressure at the sound source end P_0 are measured simultaneously. When this is done, due to the following relationship:

$$\begin{bmatrix} P_t \\ U_t \end{bmatrix} = \begin{bmatrix} D_m & B_m \\ C_m & A_m \end{bmatrix} \begin{bmatrix} P_0 \\ U_0 \end{bmatrix} \qquad \text{where} \qquad \begin{matrix} P_0/U_0 = \infty, \\ AD - BC = 1 \end{matrix}$$

the following will be obtained:

$$20 \log_{10} |P_t/P_0| = 20 \log_{10} |D_m|$$

The IL can be measured simply by the reverse arrangement method. The values in Figure 4 in the main text were obtained by this method. Although this method is not theoretically accurate due to radiation impedance and the problem of band noise, it was adopted because approximate measurements can be made simply.

APPENDIX II. SIREN PART IN PULSATING AIR FLOW TESTS

Slits were provided in the rotary disks to generate the pulsating air flow. It is conveivable that the spectrum of the exhaust sound may differ because of the shapes of these slits. In the experiments, studies were made concerning rectangular slits and round slits. Examples of this are shown in Figure 11. The dotted line in the figure is the spectrum of steady air flow at the same mean flow velocity. Naturally, the level is low, especially in the low frequency range. The upper side of the figure is the sound pressure inside the pipe at the siren outlet (exhaust pipe inlet), and the lower side is the exhaust release sound (distance of 50 cm). There are not many differences on account of the shape of the slits, although the rectangular shape has a higher level of the secondary higher harmonics (130 Hz) towards the fundamental wave (67 Hz) than the round shape. There is also a somewhat higher level in the medium frequency range. Consequently, the rectangular shape may be said to give results closer to the engine sound. The rate of the slit opening period in one opening-closing period of the siren slits (the opening time ratio) is 0.44 in the rectangular shape, and 0.67 in the round shape. In engines, the period corresponding to this is the exhaust valve opening period. In the main engines tested, th period was about 0.33 in a one-cylinder engine, and in a four-cylinder engine the sum was more than 1, indicating that one or another of the valves is open at all times.

/577

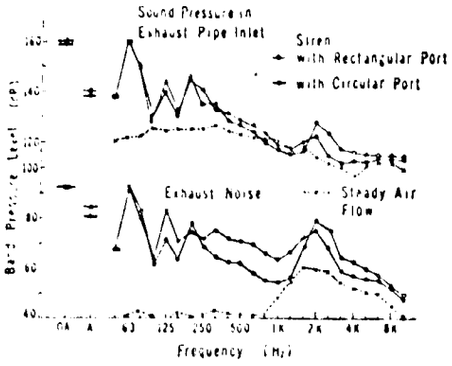

Figure 11. Noise spectrums of different types of siren port in the pulsating flow test.

APPENDIX III. PULSATING EFFECT IN THE PULSATING AIR FLOW TEST EQUIPMENT

In the pulsating air flow equipment, the air flow at the siren slit part is considered in linearized form according to the following equation:

$$\alpha A(P_1 - P_2) = U + \beta \dot{U}$$

α : flow rate coefficient

A : slit opening area

P_1: siren inlet pressure

P_2: siren outlet pressure

U : flow rate (volume velocity, exhaust direction is positive)

$\beta = \alpha \rho l_s$: coefficient for inertia effect, l_s length of slit part

Since the area A in the above equation is a pulse column, it can be expanded in Fourier series and expressed as follows:

$$A = A_0 + (1/2)A_1(e^{+j\omega t} + e^{-j\omega t}) + (1/2)A_2(e^{+j2\omega t} + e^{-j2\omega t}) + \cdots\cdots$$

The pressure and flow rate can also be expressed as follows:

$$U = U_0 + (1/2)(U_1 e^{+j\omega t} + U_1^* e^{-j\omega t}) + \cdots\cdots,$$
$$P_1 = P_{10} + (1/2)(P_{11} e^{+j\omega t} + P_{11}^* e^{-j\omega t}) + \cdots\cdots,$$
$$P_2 = P_{20} + (1/2)(P_{21} e^{+j\omega t} + P_{21}^* e^{-j\omega t}) + \cdots\cdots,$$

(The asterisks * indicate complex conjugate numbers)

In these equations, the first term on the right side represents the D.C. components, and the second term represents the fundamental frequency components of the pulse waves. Using l_1 to represent the pipe length from the pressure tank to the siren inlet, l_2 to represent the length of the exhaust pipe connected to the siren outlet, R_1 and R_2 to represent the flow resistance to the D.C. components, P_s to represent the tank pressure, P_a to represent the atmospheric pressure, R_0 to represent the characteristic

impedance of the pipe, and k as a phase constant, we can formulate the following concerning the D.C. components and the A.C. components:

$$P_s = R_s U_0 \quad P_{s0}, \quad P_s = R_s U_0 = P_{s0}$$
$$P_{11} = -jR_0 \tan(kl_1) \cdot U_1,$$
$$P_{21} = -jR_0 \tan(kl_2) \cdot U_1$$

If the above relationship is inserted into the first equation, U and P can be sought as functions of the frequency k1. The fundamental frequency component of the exhaust sound P_{s1} can be found from the following if Z_{R_s} is used as the real number component of the radiation impedance:

$$|P_{t1}|^2 = (Z_{R_s})|U_1|^2/(\cos kl_2)^2$$

If we disregard β and R and seek the above-mentioned relationship, we obtain:

$$U_0 = P\alpha A_0 \cdot (D_0/D)$$
$$U_1 = P\alpha A_1 \cdot (D_1/D)$$
$$D = \{1 + (R_0 T\alpha A_0)^2 \{1 - (1/4)(A_2/A_0)^2\}\}$$
$$D_0 = \{1 + (R_0 T\alpha A_0)^2 \{1 - (1/2)(A_1/A_0)^2 - (1/4)(A_2/A_0)^2 + (1/4)(A_1^2 A_2/A_0^3)\}\}$$
$$D_1 = \{1 - j\{(R_0 T\alpha A_0)(1 - A_2/2A_0)\}\}$$

Here,

$$P = P_s - P_{s0}, \quad T = (\tan kl_1 + \tan kl_2)$$

It is clear from these equations that, when $\tan kl_1 = \infty$, P_{11} will assume a maximum value, the phase will shift 180° away from A_1, and U_0 will assume a minimum value. It is also clear that P_{t1} will assume a minimum value. When $\tan kl_2 = \infty$, P_{21} will assume a maximum value, and the phase will be 0° U_0 will assume a minimum value, while, on the other hand, P_{t1} will assume a maximum value.

Figure 12 shows typical examples of calculations for the exhaust pipes which were tested. Here the siren opening area A is a triangular wave pulse column of the opening time ratio of 0.50. In view of its Fourier coefficients, it was assumed that $A_1/A_0 = 1.6$ and $A_2/A_0 = 0.8$. In these

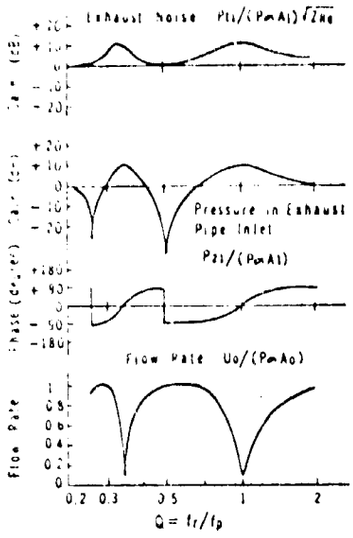

Figure 12. Pulsating effects of the exhaust pipe in the pulsating flow test system. The value Q is expressed as the ratio of the fundamental resonance frequency of exhaust pipe to the pulsating frequency.

cases, from the measured value of the mean flow velocity , 10 m/s, it was assumed that $R_0 \alpha A_0 = 0.236$ and that the pipe length ratio $\ell_2/\ell_1 = 7.3$ (R_0 is the characteristic impedance of pipe with a diameter of 3 cm). /577

On the abscissa of the graph, $Q = f_r/f_p$, where $f_r = c/4\ell_2$ and f_p is the pulse fundamental frequency.

APPENDIX IV. AERODYNAMIC NOISE

If there is a small sound source in the sound field (representative flow velocity $\bar{v}$, air flow velocity ρ, representative area A), and if the sound pressure at a point at a far distance r away from it is P, the following expressions can be stated:

Single pole sound source (boiling point) $P \propto \rho v^2 \sqrt{A}/(4\pi r)$

Two pole sound source (external force) $P \propto \rho v^3 \sqrt{A}/(C_0 4\pi r)$

Four pole sound source (stress) $P \propto \rho v^4 \sqrt{A}/(C_0^2 4\pi r)$

(The density at the measuring point is ρ_0, and the sound speed is C_0.) Consequently, since $W = (4\pi r^2)|P|^2/(\rho_0 C_0)$, the total acoustic power of the sound will be as follows:

Single pole sound source $W = K\rho^2 v^4 A/(\rho_0 C_0)$

Two pole sound source $W = K\rho^2 v^6 A/(\rho_0 C_0^3)$

Four pole sound source $W = K\rho^2 v^8 A/(\rho_0 C_0^5)$

Consequently, the following is obtained as the general equation:

$$W_n = K_n \rho^2 v^{2n} A/(\rho_0 C_0^{2n-1})$$

K is a non-dimensional coefficient.

REFERENCES

1. Harris, C. M. Handbook of Noise Control, McGraw-Hill, 1957, Chapter 21.

2. Igarashi, J. Aeron Res. Inst., University of Tokyo, 1958.

3. Fukuda and Izumi. Kikai Gakkai ronbun shū, Vol. 34, 1968, p. 1294.

4. Kanei. Kikai Gakkai ronbun shū, Vol. 26, 1960, p. 1183.

5. Fukuda. Kikai Gakkai ronbun shū, Vol. 26, 1960, p. 1167, and others.

6. Ōnaka, Nishiwaki and Hirata. Kikai Gakkai ronbun shū, Vol. 33, 1967, p. 779.

7. Coppens, A. B. J. Acous. Soc. Amer., Vol. 43, 1968, p. 516.

8. Matsuyama and Igarashi. Onkyō Gakkai kōron shū (Collection of Lecture Monographs of the Acoustical Society), October, 1969, p. 111.

9. Hirata. Onkyō Gakkai shi, Vol. 26, 1970, p. 306.

10. Martin, H. ATZ, Vol. 65, 1963, p. 281.

11. Schumacher, I. J. SAE Paper No. 771-A, 1963.

12. Martin, H. ATZ, Vol. 67, 1965, p. 293.

13. Igarashi and Fujisawa. Onkyō Gakkai kōron shū (Collection of Lecture Monographs of the Acoustical Society), November, 1966, p. 89.

14. Igarashi and Fujisawa. Onkyō Gakkai kōron shū (Collection of Lecture Monographs of the Acoustical Society), November, 1967, p. 353.

15. Martin, R. ATZ, Vol. 70, 1968, p. 90.

16. Fujimoto, Kitada and Sakurai. Onkyō Gakkai kōron shū (Collection of Lecture Monographs of the Acoustical Society), May, 1969, p. 193.

17. Fujimoto, Kitada and Sakurai. Onkyō Gakkai kōron shū (Collection of Lecture Monographs of the Acoustical Society), May, 1970, p. 179.

18. Allen, C. H. J. Acous. Soc. Amer., Vol. 31, 1959, p. 177.

19. Asanuma. Kikai Gakkai shi, Vol. 77, 1963, p. 75.

20. Yanagihara. Nainen kikan, Vol. 66, 1968, p. 11.

21. Lighthill, M. J. Pro. Roy. Soc. Lond., Series A, Vol. 211, 1952, p. 564.

22. Kotake and Okazaki. Kikai Gakkai ronbun shū, Vol. 29, 1963, p. 969.

23. Kotake and Okazaki. Kikai Gakkai shi, Vol. 67, 1964, p. 94.

24. Ising, H. Acustica, Vol. 23, 1970, p. 142.

Translated for National Aeronautics and Space Administration under contract No. NASw 2035, by SCITRAN, P.O. Box 5456, Santa Barbara, California, 93108.